Neutrino-driven explosions twenty years after SN1987A

H.-Thomas Janka, Andreas Marek and Francisco-Shu Kitaura

Max-Planck-Institute for Astrophysics, Karl-Schwarzschild-Str. 1, D-85741 Garching, Germany

Abstract. The neutrino-heating mechanism remains a viable possibility for the cause of the explosion in a wide mass range of supernova progenitors. This is demonstrated by recent two-dimensional hydrodynamic simulations with detailed, energy-dependent neutrino transport. Neutrino-driven explosions were not only found for stars in the 8–10$M_\odot$ range with ONeMg cores and in case of the iron core collapse of an $11M_\odot$ progenitor, but also for a "typical" $15M_\odot$ progenitor model. For such more massive stars, however, the explosion occurs significantly later than so far thought, and is crucially supported by large-amplitude bipolar oscillations due to the nonradial standing accretion shock instability (SASI), whose low (dipole and quadrupole) modes can develop large growth rates in conditions where convective instability is damped or even suppressed. The dominance of low-mode deformation at the time of shock revival has been recognized as a possible explanation of large pulsar kicks and of large-scale mixing phenomena observed in supernovae like SN 1987A.

Keywords: Supernovae, Nuclear aspects of supernovae
PACS: 97.60.Bw, 26.50.+x

INTRODUCTION

Besides the many other surprises Supernova 1987A brought for astronomers, it had a major impact on the theory of stellar core-collapse and explosion mainly by two discoveries. On the one hand the historical detection of two dozen neutrino events in three underground laboratories has confirmed the concept of gravitational instability and neutron star formation, in which the production of electron capture neutrinos and the emission of neutrinos and antineutrinos of all flavors by thermal processes had been predicted for a long time [1].

On the other hand, the lightcurve and spectra of SN 1987A brought unambiguous evidence that nucleosynthesis products were distributed strongly anisotropically and that large-scale mixing took place during the explosion, for which reason X-rays and γ-rays from the decay of radioactive cobalt were measured much earlier than expected. Heavy elements were observed to expand with velocities significantly larger than expected from spherically symmetric explosion models. This was interpreted as a clear sign that the onion-shell structure of the progenitor star was destroyed during the explosion [1]. Meanwhile, twenty years later, the remnant of SN 1987A at the center of the ring system reveals a clear prolate deformation and suggests a global asymmetry of the mass ejection.

Multi-dimensional supernova models showed that sufficiently strong radial mixing of radioactive nuclei requires that hydrodynamic instabilities have developed in layers near the stellar core and already during the earliest stages of the explosion. In fact, simulations of the onset of the explosion demonstrated that strong convective overturn can occur in the Ledoux-unstable region of neutrino energy deposition behind the stalled supernova shock [2, 3, 4].

Meanwhile it is clear that convection is not the only source of asymmetry during the shock stagnation phase. The standing accretion shock has been recognized to be generically unstable to nonradial deformation, even in situations where convection is damped or suppressed. This so-called "standing accretion shock instability" (SASI; [5]; for more literature, see [6]) shows a preferential growth of low shock-deformation modes (dipole, $l = 1$, and quadrupole, $l = 2$, modes in terms of an expansion in spherical harmonics). The presence of such a low-mode instability has turned out to have important implications for large-scale explosion asymmetries, pulsar kicks, and — as suggested by very recent simulations — for the development of neutrino-driven explosions. Corresponding results will be reported below and implications for SN 1987A will be discussed.

EXPLOSION MODELS WITH ENERGY-DEPENDENT NEUTRINO TRANSPORT

Numerical method

The core-collapse and post-bounce calculations presented here were performed in spherical symmetry with the neutrino-hydrodynamics code VERTEX (for details, see [7, 8]). The code module that integrates the nonrelativistic hydrodynamics equations is a conservative, Eulerian implementation of a Godunov-type scheme with higher-order spatial and temporal accuracy. The self-gravity of the stellar gas is treated with an approximation to general relativity as described in [9]. The code was tested against fully relativistic simulations in [10, 9]. The time-implicit transport routine solves the moment equations for neutrino number, energy, and momentum. It employs a variable Eddington closure factor that is obtained from iterating to convergence a simplified Boltzmann equation coupled to the set of its moment equations. The interactions of neutrinos (ν) and antineutrinos ($\bar{\nu}$) of all flavors include a state-of-the-art treatment of charged-current and neutral-current interactions with electrons, nucleons, and nuclei (making use of the improved electron capture rates on a very large NSE-ensemble of nuclei as considered by [11]). The most important neutrino-pair processes in SNe as well as reactions between neutrinos of different flavors are taken into account [8, 12]).

Neutrino-driven explosions for progenitors below $10\,M_\odot$

Recently Kitaura et al. [13] reinvestigated the stellar collapse of a $\sim 1.3\,M_\odot$ core of oxygen, neon, and magnesium, surrounded by a thin ($\sim 0.08\,M_\odot$) carbon layer and a very dilute helium shell. The progenitor had $8.8\,M_\odot$ on the main sequence mass and an initial He-core with $2.2\,M_\odot$ [14]. It can be considered as representative of the lowest-mass progenitors of core-collapse supernovae in the 8–$10\,M_\odot$ range.

Kitaura et al. obained an explosion that set in about 100 ms after core bounce and whose energy was provided by a neutrino-driven wind. The spherically symmetric (1D)

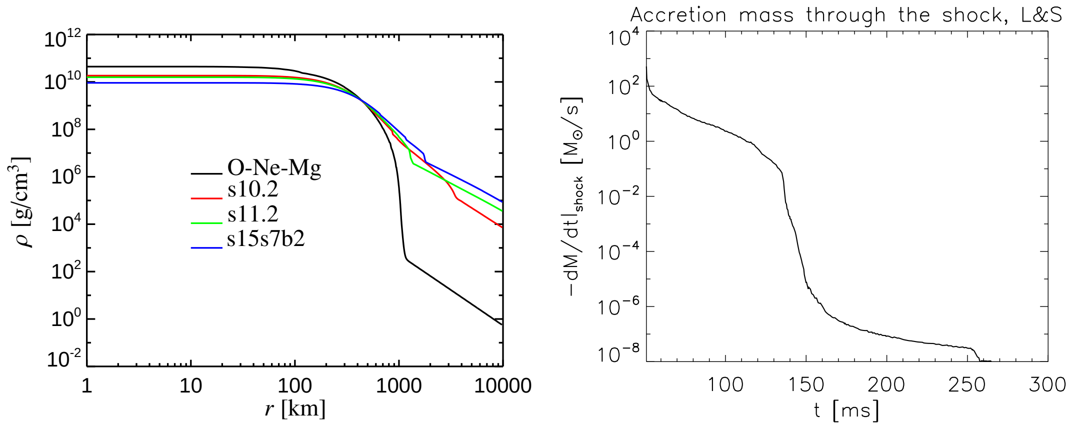

FIGURE 1. *Left:* Density profile of the ONeMg core and the surrounding He-shell of an $8.8\,M_\odot$ star, which is considered to be representative of the 8–$10\,M_\odot$ range, compared to progenitor stars with 10.2, 11.2, and $15\,M_\odot$. Note that due to the lack of data from stellar evolution models, the He-shell outside the oxygen-helium transition at about 1000 km was constructed from hydrostatic equilibrium, using a temperature profile as given by the $10.2\,M_\odot$ progenitor (A. Heger, private communication). The actual density gradient is even steeper (K. Nomoto, private communication). *Right:* The mass accretion rate of the collapsing ONeMg core at a function of time after bounce, measured just outside of the supernova shock

simulations confirm qualitatively older calculations by Mayle and Wilson [15], although the recent explosion models are significantly less powerful and important differences with respect to the nucleosynthesis conditions in the ejecta are seen.

Because of the presence of O, Ne, Mg, and C, nuclear burning still proceeds in the outer regions of the stellar core while efficient electron capture (mostly on ^{20}Ne, ^{24}Na, and ^{24}Mg) reduces the electron degeneracy pressure and drives the core to gravitational instability. It is, however, not the presence of the energy release by burning in some shells that makes the explosion of stars with such cores much easier than that of more massive progenitors with iron in the center (the compressed matter in any case is heated to nuclear statistical equilibrium, and the energy released by the burning is efficiently removed by escaping neutrinos). The main reason for the readiness of such low-mass stars to explode by the neutrino-driven mechanism is the decreasing density in the C-layer and the extremely steep density gradient at the transition from the C-shell to the He-mantle (see the left plot in Fig. 1). This leads to a continuous, fast drop of the mass accretion rate after about 50 ms of post-bounce evolution (Fig. 1, right plot). As a consequence, the stalled prompt shock starts reexpanding and accelerates the very dilute matter in its downstream region. At about 150 ms after bounce material expands outward from regions near the gain radius, where it was exposed to intense neutrino heating. This phase is associated with a steep rise of the explosion energy in Fig. 2 (right panel). Between 200 and 250 ms after bounce a powerful neutrino-driven wind begins to shed off more gas from the surface of the nascent neutron star. From this time on the explosion energy in Fig. 2 shows a more gradual but continuous further increase.

Multi-dimensional effects are obviously not crucial for obtaining neutrino-driven explosions of progenitors with the structure of the considered $\sim 9\,M_\odot$ model. Nevertheless,

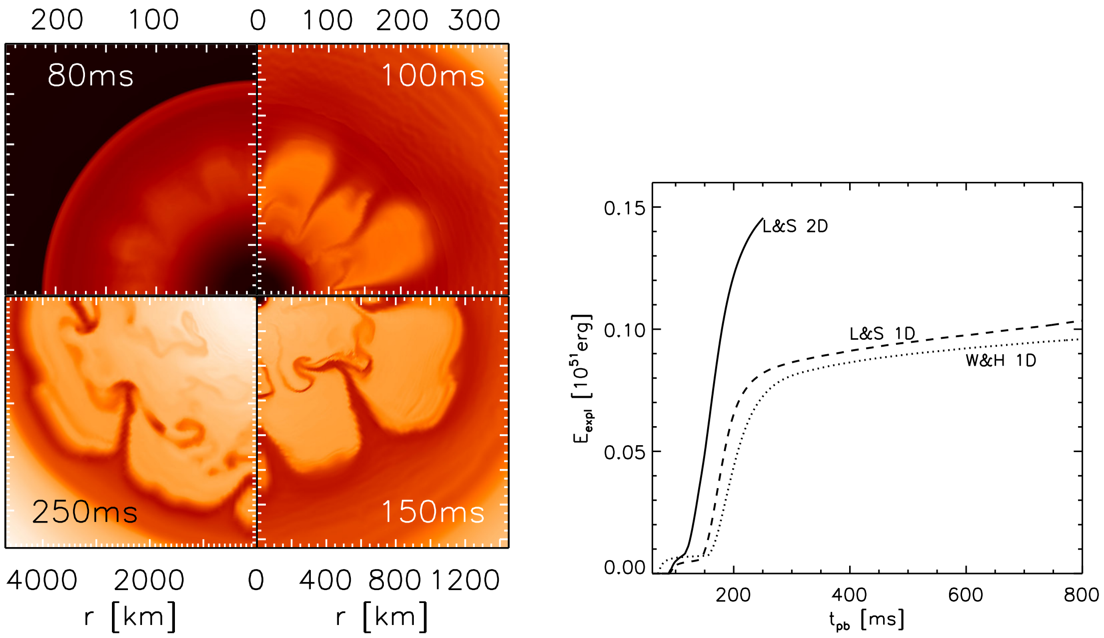

FIGURE 2. *Left:* Four snapshots of the explosion of an 8–10$M_\odot$ star in a two-dimensional (2D) simulation, which was performed in a $\pm 45°$ wedge around the equatorial plane, using periodic boundary conditions. Time is normalized to bounce. The color coding represents the entropy per nucleon with black corresponding to values of $\lesssim 7\,k_\mathrm{B}$, red to 10–15$\,k_\mathrm{B}$, orange to 15–20$\,k_\mathrm{B}$, and white to about 25$\,k_\mathrm{B}$. The supernova shock is visible as sharp red/black discontinuity at about 210 km in the upper left panel, while it is already far outside the displayed region at all other times (the corresponding shock radii are roughly 900 km, 5600 km, and 15000 km). *Right:* Explosion energy as a function of time for the 2D simulation of the left figure compared to two runs in spherical symmetry (1D) with a soft ("L&S") and a stiff ("W&H") nuclear equation of state. The steep increase of the explosion energy in the 1D models after about 150 ms is caused by the onset of the expansion of neutrino-heated matter away from the gain radius. Convective overturn leads to more efficient neutrino heating of a larger mass and to an earlier rise of the explosion energy in the 2D simulation

a simulation performed in two dimensions (2D; i.e., assuming axial symmetry) shows that convective overturn in the neutrino-heated layer between the gain radius (at 90 km) and the shock becomes strong about 80 ms after bounce and has fully developed 20 ms later (see Fig. 2, upper panels of left plot). It carries cooler matter in narrow downdrafts from larger distances to locations closer to the gain radius, where the gas is exposed to more efficient neutrino heating. Therefore a larger gas mass absorbs energy from neutrinos before it accelerates outward in rising high-entropy plumes. This leads to a considerably higher energy of the explosion than in the corresponding 1D simulations (Fig. 2, right plot), but has essentially no effect on the propagation of the supernova shock during this phase, because the shock is already far outside of the convective region. After about 150 ms of post-bounce evolution the radial propagation of the neutrino-heated layers has become so fast that the mixing motions freeze out and the corresponding fluid pattern with characteristic Rayleigh-Taylor mushrooms expands self-similarly with high velocity (Fig. 2, lower panels in the left plot).

The 2D simulation also shows that convection inside the nascent neutron star does

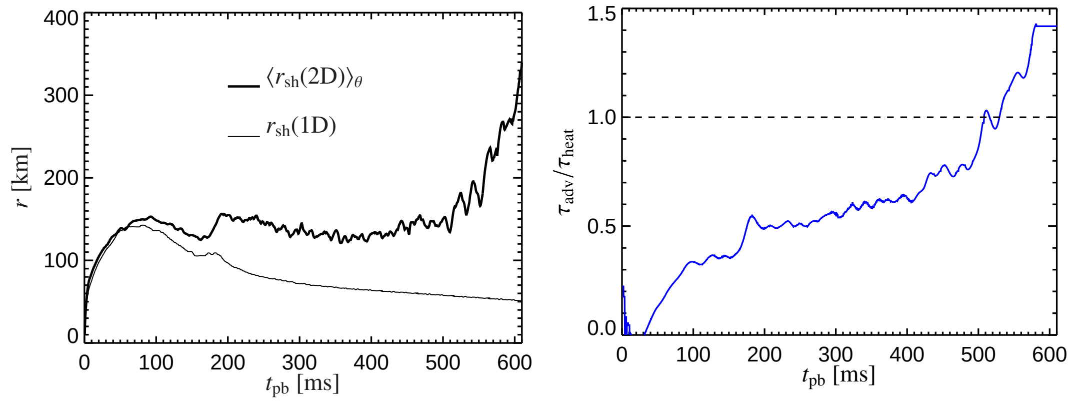

FIGURE 3. *Left:* Angular average of the shock radius (volume weighted) for the 2D simulation of the $15M_\odot$ explosion compared to the shock position of a corresponding spherically symmetric simulation. *Right:* Evolution of the ratio of advection timescale of accreted matter through the gain layer to the neutrino-heating timescale for the exploding $15M_\odot$ model. There is a continuous increase until the critical value of unity is exceeded after about 500 ms of post-bounce evolution. At $t > 580$ ms the beginning strong overall expansion of the postshock layer prevents a reasonable determination of the advection timescale

not lead to any significant increase of the neutrino luminosities and thus of the neutrino heating behind the shock. The enhanced explosion energy is merely a consequence of the convective activity behind the supernova shock. This is clearly different from the simulations by Mayle & Wilson [15], who obtained models with larger explosion energy by assuming that the neutrino luminosities were boosted by neutron-finger convection below the neutrinosphere.

The rapid outward acceleration also has the consequence that the convective pattern never develops dominant power on the largest scales. The expansion of the gain layer happens so quickly that the convective plumes have no time to merge to structures with lateral wavelengths of more than about 45°. Since the shock radius grows continuously with time, also the SASI has no possibility to grow (for more details, see below). Such a situation disfavors the development of a large global asymmetry of the small amount of material that is accelerated during the early stages of the explosion. Therefore the pulsar kick velocities must be expected to remain rather small (roughly $\lesssim 100$ km/s) in case of the O-Ne-Mg core collapse events.

SASI-supported neutrino-driven explosions of stars above $10M_\odot$

The core structure of stars more massive than about $10M_\odot$ is considerably different from that of lower mass supernova progenitors (see Fig. 1). Spherically symmetric calculations, carried out over many hundreds of milliseconds after core bounce, have therefore not found explosions happening. Instead, the supernova shock stalls and mass is continuously accreting onto the forming neutron star (see the 1D result in the left plot of Fig. 3).

Hydrodynamic instabilities in the supernova core, however, can change the situation. In 2D simulations Buras et al. [16] obtained an explosion of an $11.2M_\odot$ progenitor.

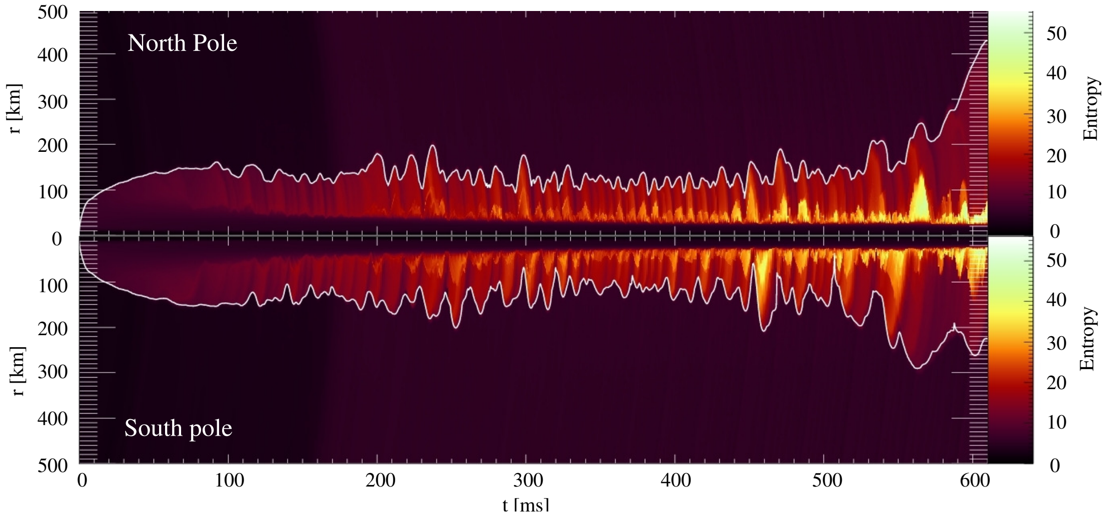

FIGURE 4. Radial positions of the shock near the north and south pole as functions of post-bounce time (white lines) in the 2D simulation of the explosion of a $15M_{\odot}$ star. The color coding represents the entropy per nucleon of the stellar gas. The quasi-periodic shock expansion and contraction due to the SASI can be clearly seen

Numerical tests with different angular wedges and lateral boundary conditions of the polar grid showed that the crucial difference here was the growth of low ($l = 1, 2$) SASI modes. The associated development of large-amplitude bipolar oscillations pushed the shock to larger radii and thus increased the timescale of accreted matter to fall from the shock (at $R_{\rm s}$) to the gain radius $R_{\rm g}$. The corresponding advection timescale

$$\tau_{\rm adv} \equiv \frac{R_{\rm s} - R_{\rm g}}{|\langle v_r \rangle|} \tag{1}$$

can be considered as a measure of the duration gas is exposed to neutrino heating in the gain layer. When the stalled shock reaches a larger radius $R_{\rm s}$, the preshock velocity and average postshock velocity $\langle v_r \rangle$ are significantly smaller, which leads to a considerably longer advection timescale (roughly $\tau_{\rm adv} \propto R_{\rm s}^{3/2}$; Eq. (15) in [17]). Our numerical experiments showed that the presence of postshock convection alone (if the low SASI modes were suppressed by grid constraints) was unable to provide enough support for a neutrino-driven explosion. When SASI oscillations helped increasing the shock radius, however, the crucial ratio of advection timescale to neutrino heating timescale grows and finally exceeds the critical value of unity. The neutrino heating timescale,

$$\tau_{\rm heat} \equiv \frac{E_{\rm bind}[R_{\rm gain}, R_{\rm shock}]}{Q_{\rm heat}} \tag{2}$$

measures the time it takes neutrinos to deposit (with an integrated rate $Q_{\rm heat}$) and energy equal to the binding energy $E_{\rm bind}[R_{\rm gain}, R_{\rm shock}]$ of the matter in the gain layer.

Very recent simulations show that such a positive feedback between low-mode SASI oscillations and neutrino heating also occurs in a $15M_{\odot}$ progenitor (model s15s7b2

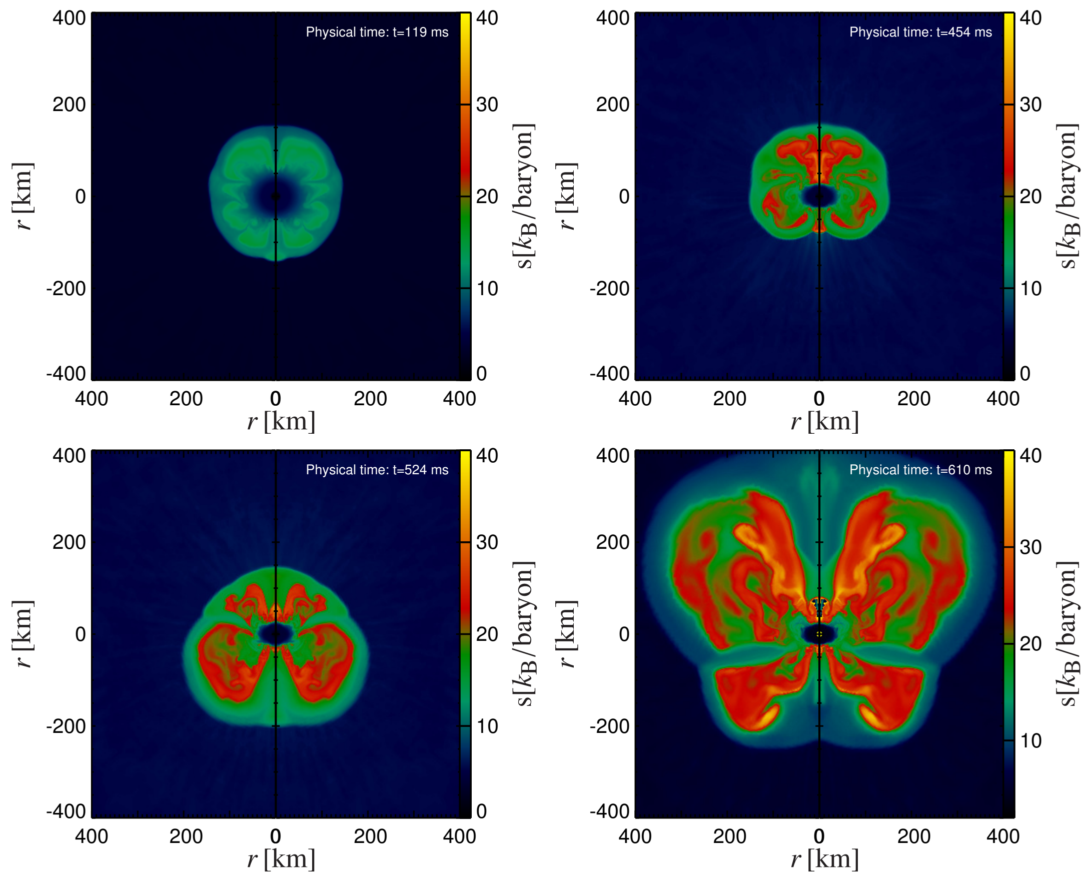

FIGURE 5. Four snapshots from the post-bounce evolution of the exploding $15M_\odot$ star in a 2D simulation. The upper left plot shows the entropy distribution at $t = 119$ms after bounce, about 40 ms after the postshock convection has reached the nonlinear regime. The upper right and lower left plots ($t = 454$ms and $t = 524$ms after bounce) demonstrate the presence of a very strong bipolar oscillation due to the SASI, and the lower right plot ($t = 610$ms p.b.) displays the acceleration phase of the strongly aspherical explosion with a large $l = 1$ component. Note that the contracting nascent neutron star exhibits a growing prolate deformation because of the rotation assumed in this simulation

of [18]). Also there it finally leads to a neutrino-driven explosion, however at much a later time after core bounce (Fig. 3). The particular model considered here includes a modest amount of rotation (the pre-collapse iron core had a rotation period of about 12 seconds as in Sect. 3.4 of [16]), which explains a growing oblateness of the nascent neutron star (see Fig. 5). Comparison with non-rotating models, however, reveals that angular momentum dependent effects may cause some quantitative differences (and may to some extent foster the evolution towards an explosion) but do not seem to be the essential ingredient that determines the overall behavior of the collapsing stellar core in

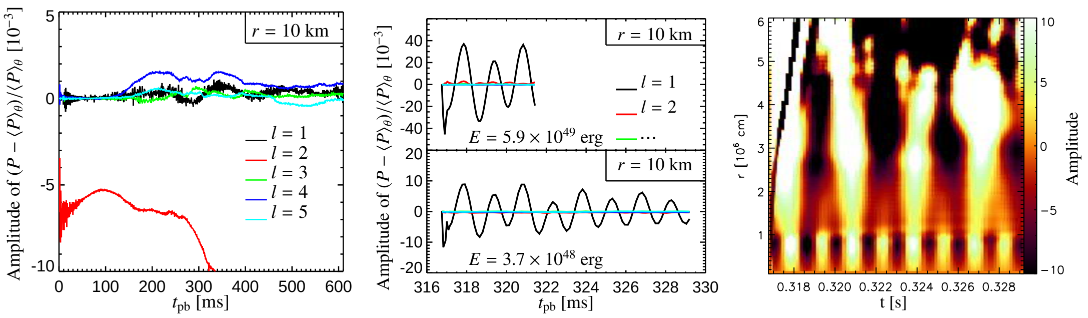

FIGURE 6. *Left:* G-mode oscillations of the nascent neutron star in the exploding $15M_\odot$ simulation during 610 ms of post-bounce evolution. The plot shows the amplitudes of the $l = 1$ to $l = 5$ modes of the pressure fluctuations at a radius of $r = 10$ km expanded in spherical harmonics. Note that the quadrupole mode ($l = 2$) has a large and growing amplitude because of the oblateness of the rotating neutron star. *Middle:* Test simulations with artificially instigated dipole ($l = 1$) oscillation of the neutron star. Two different amplitudes of the initially imposed velocity field were used, 5×10^7 cm/s and 2×10^8 cm/s, corresponding to a factor of 16 different kinetic energies (as indicated in the plot). The clear presence of many cycles of the dipole oscillation demonstrates the ability of our numerical code to follow such gravity waves, if they are excited. *Right:* The amplitude of the $l = 1$ mode in the lower panel of the middle plot as function of time and radius. Interior of about 10 km the core oscillates with twice the frequency as the mantle outside of $r \approx 25$ km. In the intermediate, convective layer the gravity waves are damped

the long run[1].

Figure 3 (left) reveals a growth of the average shock radius, which starts at about 350 ms after bounce and is accompanied by a continuous rise of the timescale ratio $\tau_{\mathrm{adv}}/\tau_{\mathrm{heat}}$ (Fig. 3, right). This rise is caused by an increase of the average advection timescale τ_{adv}, while τ_{heat} remains nearly constant. The kinetic energy (also for the lateral component of the velocity) in the gain layer triples during this period of the evolution (while the rotational energy changes only by a modest amount), suggesting that nonradial fluid motions become more and more violent during this phase. Indeed, the bipolar SASI oscillations, which are visible from alternating shock expansion and contraction phases in the northern and southern hemispheres with a period of 10–15 ms, exhibit a growing amplitude for $t_{\mathrm{pb}} > 350$ ms (Fig. 4). With a larger average shock radius also more mass is accumulated in the gain layer. At $t \gtrsim 530$ ms the critical timescale ratio exceeds unity and a runaway situation is reached. The accelerating overall expansion indicates the onset of a strongly aspherical, neutrino-powered explosion (Fig. 5).

Some comments on core g-modes and the acoustic mechanism

In view of the recent numerical finding of acoustically-driven explosions, which are initiated by the acoustic power generated by large-amplitude core g-mode oscillations of

[1] Because of the considerable CPU-time requirements of 2D simulations with our sophisticated, energy-dependent neutrino transport, we could not yet carry the comparative runs of non-rotating models to the very late post-bounce time reached in the case presented here.

the accreting neutron star [19, 20], we have evaluated our long-time $15\,M_\odot$ simulation for the gravity-wave activity of the forming compact remnant. Figure 6 (left) displays the g-mode amplitudes of the first terms ($l = 1, ..., 5$) of a spherical harmonics expansion of the pressure fluctuations at a radius of 10 km inside the neutron star. The analysis follows the description in Ref. [19], see Fig. 7 there. The amplitudes of core g-modes in our model are roughly two orders of magnitude smaller than those seen in the run-up to an explosion in that figure. The acoustic energy flux radiated by the oscillating neutron star in our model is therefore completely negligible compared to neutrino heating behind the shock, which typically deposits energy at a net rate of $3\text{–}4\times10^{51}$ erg/s at $t > 200$ ms after bounce. The acoustic mechanism does not play a role for the evolution of our model and, according to the simulations in[20], it might become relevant only much later than our model explodes by neutrino-energy deposition.

But is our code able to follow core g-mode oscillations, in particular of $l = 1$ type, because in this case the gas in the stellar center participates in the motion? The answer is "yes" (in contrast to statements that can be found in the literature[2], see [19, 20]). The middle and right panels of Figure 6 show results of test simulations in which at some moment of the post-bounce evolution we artificially instigated a large dipole g-mode by imposing an $l = 1, n = 1$ (i.e., we assumed one radial node) perturbation of the z-component of the velocity field with varied amplitude and conserved linear momentum. The plots demonstrate that essentially a pure $l = 1$ oscillation develops (after some initial relaxation, because our chosen perturbation did not correspond to an eigenfunction), which the code is able to follow through many cycles. We are therefore confident that we should see large core g-mode oscillations, if the anisotropic accretion flow around the neutron star were causing their excitation.

CONCLUSIONS

The results of 2D supernova simulations presented in this paper demonstrate the ability of neutrino heating to initiate delayed explosions for progenitors in a wider range of masses. The explosion occurs significantly later than observed in older calculations with approximative neutrino transport. We identified large-amplitude SASI modes to play a crucial, supportive role for the development of the explosion because they enforce shock expansion and thus reduce the average infall velocity in the postshock region, which enables the accreted matter to stay in the neutrino-heating layer for a significantly longer time.

Our simulations, however, were stopped too early (for CPU time reasons) to allow for a final determination of the explosion energy. Accretion of matter by the shock is still going on, in particular in the 11 and $15\,M_\odot$ stars, and gas is channelled towards the gain radius, where neutrino heating is strongest. A large fraction of this infalling material

---

[2] It is true that in our simulations a few radial zones in the central $\sim$1.5 km of the star are treated in spherical symmetry to get around the most severe CFL constraint for the hydrodynamic timestep. This small central region within a protoneutron star of radius 15–50 km, however, resembles a pinhead in the middle of a cup filled with sloshing tea.

will start reexpanding, and energy this gas has absorbed from neutrinos and is released by nucleon recombination to alpha particles and iron-group nuclei will contribute to the explosion energy. In order to obtain reliable numbers for the explosion properties, the simulations will have to follow this accretion phase, which might last even for hundreds of milliseconds. Ultimately, however, 3D simulations will be needed. The explosion, its onset and strength, may depend on the additional degrees of freedom that are accessible to the fluid flow in three dimensions. Convective downdrafts and buoyant plumes, vorticity, and spiral modes are different in 3D or even do not exist when the flow is constrained to axisymmetry with all structures being tori around the polar grid axis.

The kind of asphericities seen in case of our 11.2 and $15\,M_\odot$ explosion models, with a large contribution from an $l=1$ component, were shown to lead to such a big anisotropy of the supernova mass ejection that the neutron star receives a recoil sufficiently strong to explain the high velocities observed for many young pulsars, even those in excess of 1000 km/s [21, 22]. Moreover, the initial deformation of the supernova shock and the asymmetric ejecta distribution are the seed of subsequent hydrodynamic instabilities at the composition interfaces of the disrupted star after the passage of the supernova shock. These instabilities prevent the strong deceleration of the heavy elements and lead to a highly anisotropic distribution not only of Fe-group nuclei but also of silicon and oxygen. Large-scale mixing takes place, in course of which hydrogen and helium are carried deep into the star and pockets and clumps of heavy elements remain expanding with high velocities as observed in SN 1987A [23].

Even 20 years after the spectacular stellar death it is not clear what caused the explosion of SN 1987A. The ring system was interpreted as a sign for rapid rotation being present in the $\sim 18\,M_\odot$ progenitor star. In particular the existence of a common axis of the ring system and of the elongated ejecta is a strong indication that rotation has played a role in the dying star, possibly as the consequence of a binary merger event some ten thousand years before the stellar collapse (see P. Podsiadlowski's talk at this meeting). It is, however, not clear how such a merger has affected the angular momentum evolution of the stellar core. Only if the initial spin period of the core was small ($\lesssim 2$ s according to Ref. [24]), the free energy of rotation in the nascent neutron star was sufficiently large to power a supernova explosion by magnetohydrodynamic effects. But if the collapsing core was rotating so rapidly, why then is there no sign now of the energy input from a bright, Crab-like pulsar? A delayed collapse of a transiently existing neutron star to a black hole is disfavored as the solution of this puzzle, because the compact remnant formed in a typical SN 1987A progenitor is not expected to be so heavy that it cannot be stabilized by nuclear equation-of-states that are consistent with measured neutron star masses. Moreover, the pronounced prolate deformation of the now visible supernova ejecta at the center of the ring system may not be an unambiguous signature of very rapid core rotation but could result from a bipolar SASI asymmetry. SN 1987A may not only have been a unique event, it may also have been an uncommon one. We will probably never find out with final certainty. The next galactic supernova, however, will give us a new chance to learn more about the processes that trigger the explosion of a massive star: Tens of thousands of neutrino events will be captured by various underground experiments, and highly sensitive instruments promise to register the gravitational-wave signal produced by a nonspherical bounce and by hydrodynamic instabilities in the supernova core.

ACKNOWLEDGMENTS

We are very grateful to R. Buras, W. Hillebrandt, K. Kifonidis, B. Müller, E. Müller, and M. Rampp for their input to various aspects of the reported project, and A. Heger, K. Nomoto, and S. Woosley for data of their progenitor models. This work was supported by the Deutsche Forschungsgemeinschaft through the Transregional Collaborative Research Center SFB/TR 27 "Neutrinos and Beyond", the Collaborative Research Center SFB-375 "Astro-Particle Physics", and the Cluster of Excellence "Origin and Structure of the Universe" (`http://www.universe-cluster.de`). Supercomputer time grants at the John von Neumann Institute for Computing (NIC) in Jülich, at the High Performance Computing Center Stuttgart (HLRS) of the University of Stuttgart, and at the Computer Center in Garching (RZG) are acknowledged.

REFERENCES

1. W.D. Arnett, J.N. Bahcall, R.P. Kirshner, and S.E. Woosley, *Annu. Rev. Astron. Astrophys.* **27**, 629–700 (1989).
2. M. Herant, W. Benz, W.R. Hix, C.L. Fryer, and S.A. Colgate, *Astrophys. J.* **435**, 339–361 (1994).
3. A. Burrows, J. Hayes, and B.A. Fryxell, *Astrophys. J.* **450**, 830–850 (1995).
4. H.-T. Janka, and E. Müller, *Astron. Astrophys.* **306**, 167–198 (1996).
5. J.M. Blondin, A. Mezzacappa, and C. DeMarino, *Astrophys. J.* **584**, 971–980 (2003).
6. L. Scheck, H.-T. Janka, T. Foglizzo, and K. Kifonidis, *Astron. Astrophys.*, submitted; arXiv:0704.3001.
7. M. Rampp, and H.-T. Janka, *Astron. Astrophys.* **396**, 361–392 (2002).
8. R. Buras, M. Rampp, H.-T. Janka, and K. Kifonidis, *Astron. Astrophys.* **447**, 1049–1092 (2006).
9. A. Marek, H. Dimmelmeier, H.-T. Janka, E. Müller, and R. Buras, *Astron. Astrophys.* **445**, 273–289 (2006).
10. M. Liebendörfer, M. Rampp, H.-T. Janka, and A. Mezzacappa, *Astrophys. J.* **620**, 840–860 (2005).
11. K. Langanke, G. Martínez-Pinedo, J.M. Sampaio, D.J. Dean, W.R. Hix, O.E.B. Messer, A. Mezzacappa, M. Liebendörfer, H.-T. Janka, and M. Rampp, *Phys. Rev. Lett.* **90**, 241102 (2003).
12. A. Marek, H.-Th. Janka, R. Buras, M. Liebendörfer, and M. Rampp, *Astron. Astrophys.* **443**, 201–210 (2005).
13. F.S. Kitaura, H.-T. Janka, and W. Hillebrandt, *Astron. Astrophys.* **450**, 345–350 (2006).
14. K. Nomoto, *Astrophys. J.* **277**, 791–805 (1984).
15. R. Mayle, and J.R. Wilson, *Astrophys. J.* **334**, 909–926 (1988).
16. R. Buras, H.-T. Janka, M. Rampp, K. Kifonidis, *Astron. Astrophys.* **457**, 281–308 (2006).
17. H.-T. Janka, K. Kifonidis, and M. Rampp, "Supernova Explosions and Neutron Star Formation", in *Physics of Neutron Star Interiors*, edited by D. Blaschke, N.K. Glendenning, and A. Sedrakian, Springer, Berlin, 2001, pp. 333–363; astro-ph/0103015.
18. S.E. Woosley, and T.A. Weaver, *Astrophys. J. Suppl.* **101**, 181–235 (1995).
19. A. Burrows, E. Livne, L. Dessart, C.D. Ott, and J. Murphy, *Astrophys. J.* **640**, 878–890 (2006).
20. A. Burrows, E. Livne, L. Dessart, C.D. Ott, and J. Murphy, *Astrophys. J.* **655**, 416–433 (2007).
21. L. Scheck, T. Plewa, H.-T. Janka, K. Kifonidis, and E. Müller, *Phys. Rev. Lett.* **92**, 011103 (2004).
22. L. Scheck, K. Kifonidis, H.-T. Janka, and E. Müller, *Astron. Astrophys.* **457**, 963–986 (2006).
23. K. Kifonidis, T. Plewa, L. Scheck, H.-T. Janka, and E. Müller, *Astron. Astrophys.* **453**, 661–678 (2006).
24. A. Burrows, L. Dessart, E. Livne, C.D. Ott, and J. Murphy, *Astrophys. J.*, submitted; astro-ph/0702539.